

Dual fermion approach to nonlocal correlations in the Hubbard model

A. N. Rubtsov,¹ M. I. Katsnelson,² and A. I. Lichtenstein³

¹*Department of Physics, Moscow State University, 119992 Moscow, Russia*

²*Institute for Molecules and Materials, Radboud University, 6525 ED Nijmegen, The Netherlands*

³*Institute of Theoretical Physics, University of Hamburg, 20355 Hamburg, Germany*

A new diagrammatic technique is developed to describe nonlocal effects (e.g., pseudogap formation) in the Hubbard-like models. In contrast to cluster approaches, this method utilizes an exact transition to the dual set of variables, and it therefore becomes possible to treat the irreducible vertices of an effective *single-impurity* problem as small parameters. This provides a very efficient interpolation between weak-coupling (band) and atomic limits. The antiferromagnetic pseudogap formation in the Hubbard model is correctly reproduced by just the lowest-order diagrams.

PACS numbers: 71.10.Fd, 71.27.+a, 05.30.Fk

Lattice fermion models with strong a local interaction (Hubbard-like models [1]) are believed to catch the basic physics of various systems, such as high-temperature superconductors [2, 3], itinerant-electron magnets [4], Mott insulators [5], ultracold atoms in optical lattices [6], etc. Unfortunately, the analytical treatment of these problems is essentially restricted by the lack of explicit small parameters for the most physically interesting interactions. Direct numerical methods, such as exact diagonalization [7] or quantum Monte Carlo (QMC) [8, 9] are limited by the clusters being of a relatively small size, or face other obstacles such as the famous sign problem for QMC simulations at low temperature [10]. There is a very successful approximate way to treat these models via the framework of so-called dynamical mean-field theory (DMFT) [5], where the lattice many-body problem is replaced with an effective impurity model. This approach is essentially based on the assumption of a local (i.e. momentum-independent) fermionic self energy. Indeed, there are numerous interesting phenomena which are basically determined by *local* electron correlations, such as Kondo effect [11], Mott-Hubbard transitions [5] and local moment formation in itinerant-electron magnets [12]. At the same time, momentum dependence of the self energy is of crucial importance for Luttinger liquid formation in low-dimensional systems [3, 13], d-wave pairing in high- T_c superconductors [2, 14, 15], and non-Fermi-liquid behavior due to van Hove singularities in two dimensions [16]. Recently a rather strong momentum dependence of the effective mass renormalization in photoemission spectra of iron was observed [17].

Currently, non-local many body effects in strongly correlated systems are mainly studied via the framework of various cluster generalizations of DMFT [14, 15, 18, 19]. Cluster methods do catch basic physics of d-wave pairing and antiferromagnetism in high- T_c superconductors [14, 15], and the effects of intercrite Coulomb interaction in various transition-metal oxides [20, 21, 22]. At the same time, however effects like Luttinger liquid formation or van Hove singularities can not be described in cluster approaches. In such cases the correlations are essentially

long-ranged and it is more natural to describe the correlations in momentum space. Recently attempts have been made to consider non local correlation effects in momentum space starting from DMFT as a zeroth-order approximation [23, 24]. This approach requires a solution of ladder-like integral equation for complete vertex Γ and the subsequent use of the Bethe-Salpeter equation to obtain Green's functions. The first step here exploits an irreducible vertex of the effective impurity problem $\gamma^{(4)}$, whereas the second step uses just the bare interaction parameter U . This second step makes the generalized DMFT approach mostly suitable to the weak-coupling regime [25].

In this Letter, we present a scheme which is accurate in both small- U and large- U limits and does not require numerically expensive solutions of any integral equations. A comparison of the results with lattice QMC simulations for the two-dimensional (2D) Hubbard model in the pseudogap regime demonstrates that the scheme is actually accurate even in the less-favorable case of intermediate U .

We proceed with 2D Hubbard model with the corresponding imaginary-time action

$$S[c, c^*] = \sum_{\omega k \sigma} (\epsilon_k - \mu - i\omega) c_{\omega k \sigma}^* c_{\omega k \sigma} + U \sum_i \int_0^\beta n_{i\uparrow\tau} n_{i\downarrow\tau} d\tau. \quad (1)$$

Here β and μ are the inverse temperature and chemical potential, respectively, $\omega = (2j+1)\pi/\beta$, $j = 0, \pm 1, \dots$ are the Matsubara frequencies, $\sigma = \uparrow, \downarrow$ is the spin projection. The bare dispersion law is $\epsilon_k = -2t(\cos k_x + \cos k_y)$, c^* , c are the Grassmannian variables, $n_{i\sigma\tau} = c_{i\sigma\tau}^* c_{i\sigma\tau}$, where the indices i and k label sites and quasi-momenta.

In the spirit of DMFT, we introduce a single-site reference system (an effective impurity model) with the action

$$S_{imp} = \sum_{\omega, \sigma} (\Delta_\omega - \mu - i\omega) c_{\omega, \sigma}^* c_{\omega, \sigma} + U \int_0^\beta n_{\uparrow\tau} n_{\downarrow\tau} d\tau \quad (2)$$

where Δ_ω is as an yet undefined hybridization function describing the interaction of the effective impurity with

a bath. We suppose that all properties of the impurity problem are known, so that its single-particle Green's function g_ω is known, and the irreducible vertex parts $\gamma^{(4)}, \gamma^6$, etc. Our goal is to express the Green's function $G_{\omega k}$ and vertices Γ of the lattice problem in Eq.(1) via these quantities.

We utilize a dual transformation to the set of new Grassmannian variables f, f^* . The following identity

$$e^{A^2 c_{\omega k \sigma}^* c_{\omega k \sigma}} = B^{-2} \int e^{-AB(c_{\omega k \sigma}^* f_{\omega k \sigma} + f_{\omega k \sigma}^* c_{\omega k \sigma}) - B^2 f_{\omega k \sigma}^* f_{\omega k \sigma} df_{\omega k \sigma}^* df_{\omega k \sigma}}, \quad (4)$$

is valid for arbitrary complex numbers A and B . We chose $A^2 = (\Delta_\omega - \epsilon_k)$ and $B^2 = g_\omega^{-2}(\Delta_\omega - \epsilon_k)^{-1}$ for each set of indices ω, k, σ .

With this identity, the partition function of the lattice problem $Z = \int e^{-S[c, c^*, f, f^*]} \mathcal{D}c^* \mathcal{D}f \mathcal{D}c \mathcal{D}f^*$, where

$$S[c, c^*, f, f^*] = \sum_i S_{imp}[c_i, c_i^*] + \sum_{\omega k \sigma} [g_\omega^{-1}(f_{\omega k \sigma}^* c_{\omega k \sigma} + c_{\omega k \sigma}^* f_{\omega k \sigma}) + g_\omega^{-2}(\Delta_\omega - \epsilon_k)^{-1} f_{\omega k \sigma}^* f_{\omega k \sigma}] \quad (5)$$

and Z_f is a product $\prod_{\omega k} g_\omega^2(\Delta_\omega - \epsilon_k)$.

As a next step, we establish an exact relation between the Green's function of the initial system $G_{\tau-\tau', i-i'} = -\langle T c_{\tau i} c_{\tau' i'}^* \rangle$ and that of the dual system $G_{\tau-\tau', i-i'}^{dual} = -\langle T f_{\tau i} f_{\tau' i'}^* \rangle$. To this aim, we can replace $\epsilon_k \rightarrow \epsilon_k + \delta\epsilon_{\omega k}$ with a differentiation of the partition function with respect to $\delta\epsilon_{\omega k}$. Since we have two expressions for the action (1) and (5), one obtains

$$G_{\omega, k} = g_\omega^{-2}(\Delta_\omega - \epsilon_k)^{-2} G_{\omega, k}^{dual} + (\Delta_\omega - \epsilon_k)^{-1}, \quad (6)$$

where the last term follows from the differentiation of Z_f .

The crucial point is that the integration over the initial variables c_i^*, c_i can be performed separately for each lattice site, since $\sum_k (f_k^* c_k + c_k^* f_k) = \sum_i (f_i^* c_i + c_i^* f_i)$. For a given site i , one should integrate out c_i^*, c_i from the action that equals $S_{site}[c_i, c_i^*, f_i, f_i^*] = S_{imp}[c_i, c_i^*] + \sum_\omega g_\omega^{-1}(f_\omega^* c_\omega + c_\omega^* f_\omega)$. We obtain

$$\int e^{-S_{site}} \mathcal{D}c_i^* \mathcal{D}c_i = Z_{imp} e^{\sum_\omega g_\omega^{-1} f_{\omega i \sigma}^* f_{\omega i \sigma} - V[f_i, f_i^*]}, \quad (7)$$

where Z_{imp} is a partition function of the impurity problem (2). The Taylor series for $V[f_i, f_i^*]$ in powers of f_i, f_i^* starts from $-\gamma_{1234}^{(4)} f_1^* f_2 f_3 f_4$ (indices stand for a combination of σ and ω , for example f_1^* means f_{σ_1, ω_1}^*). Further Taylor series terms yield similar combinations including $\gamma^{(n)}$ of higher orders.

We arrive with an action S depending on the new variables f, f^* only:

$$S[f, f^*] = \sum_{\omega k \sigma} g_\omega^{-2} ((\Delta_\omega - \epsilon_k)^{-1} + g_\omega) f_{\omega k \sigma}^* f_{\omega k \sigma} + \sum_i V_i, \quad (8)$$

Since Δ is independent of k , the action (1) can be represented in the form

$$S[c, c^*] = \sum_i S_{imp}[c_i, c_i^*] - \sum_{\omega k \sigma} (\Delta_\omega - \epsilon_k) c_{\omega k \sigma}^* c_{\omega k \sigma}. \quad (3)$$

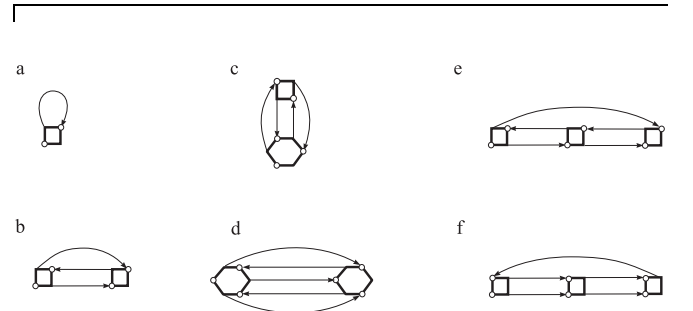


FIG. 1: Various diagrams for Σ^{dual} .

with $V_i \equiv V[f_i^*, f_i]$. In this dual action, the interaction terms remain localized in space, but are non-local in imaginary time, since, for example $\gamma^{(4)}$ depends on the three independent Matsubara frequencies. To obtain the dual potential V for a practical calculation, one should solve then the impurity problem (2).

Finally a regular diagrammatic expansion in powers of V can be performed. In these diagrams, the lines are $G_{\omega k}^{dual}$, whereas the vertices are $\gamma^{(n)}$. The rules of diagram construction are very similar to usual ones, but the six-leg and higher-order vertices appear because $\gamma^{(6)}$ and higher terms are present in the series for V . Figure 1 shows several diagrams contributing dual self-energy $\Sigma_{\omega, k}^{dual} = -[(\Delta_\omega - \epsilon_k)^{-1} g_\omega^{-2} + g_\omega^{-1} + (G_{\omega, k}^{dual})^{-1}]$.

It is important to understand what can be a small parameter in such an expansion. Clearly, if U is small, then $\gamma^{(4)} \propto U$, $\gamma^{(6)} \propto U^2$ etc., and in the weak-correlated regime vertices in the diagrams will be small (Fig. 1), and higher-order vertices will be even smaller.

At this point we establish a condition for Δ , which was so far an arbitrary quantity. We use a self-consistent

condition

$$\sum_k \frac{1}{g_\omega + (\Delta_\omega - \epsilon_k)^{-1}} = 0. \quad (9)$$

It is easy to show that this is exactly equivalent to the DMFT equation for the “hybridization function” Δ_ω [5]. In terms of the dual variables (8), this condition means that local part of the bare dual Green’s function equals zero. In particular, this leads to the vanishing of the first-order “Hartree” corrections in the diagrammatic expansion. Another important consequence of this choice is that the bare dual Green’s function turns out to be quasi-local and small near the atomic limit ($\epsilon_k \ll U$). This ensures the fast convergence of new diagrammatic expansion in the strong-coupling limit.

The simplest contribution to the dual self energy is given by the diagram (b) from Figure 1. All other diagrams are smaller both in the strong-coupling and weak-coupling regime, due to extra vertices or extra lines, respectively.

On general grounds [26, 27, 28], it is more correct to reformulate the diagrammatic expansion in terms of skeleton diagrams. That is, in terms of the renormalized G^{dual} rather than its bare value. In this case the “Hartree” diagram (a) in Figure 1 is no longer equal to zero. Thus, it is natural to expect that diagrams (a) and (b) provide the main corrections to the DMFT in the whole range of parameters. It is worth also mentioning that the contribution (a) is local and diagram (b) gives the main k -dependent contribution to the self energy.

Practically, the calculation was organized as follows. The effective impurity DMFT problem was solved by the continuous-time QMC code [30]. In the last DMFT-run, the vertices γ have been produced. We then calculated Σ^{dual} by the following iterative procedure: we started with the bare dual Green’s function and estimated the diagrams (a) and (b) from Figure 1. This gives Σ^{dual} and G^{dual} for the next iteration. Typically, about 10 iterations are enough to ensure convergence. Finally, the self energy and Green’s function of the initial system (1) was restored via Eq.(6).

As the most challenging test, we performed the calculation for the half-filled square-lattice Hubbard model, at U equal the bandwidth $8|t|$. There are strong antiferromagnetic fluctuations in the system, although true antiferromagnetism is impossible at finite temperature in the 2D system with an isotropic order parameter [29]. Consequently, the temperature decrease results in a formation of an antiferromagnetic pseudogap. In order to obtain reference point for a further comparison with the results of our new approximation scheme, we performed a direct lattice QMC calculation with the continuous-time QMC code [30]. A formation of the pseudogap was observed with a lower pseudogap for lower temperatures. It was also noticed that the local part of self-energy did not change much with temperature, while the nonlocal part

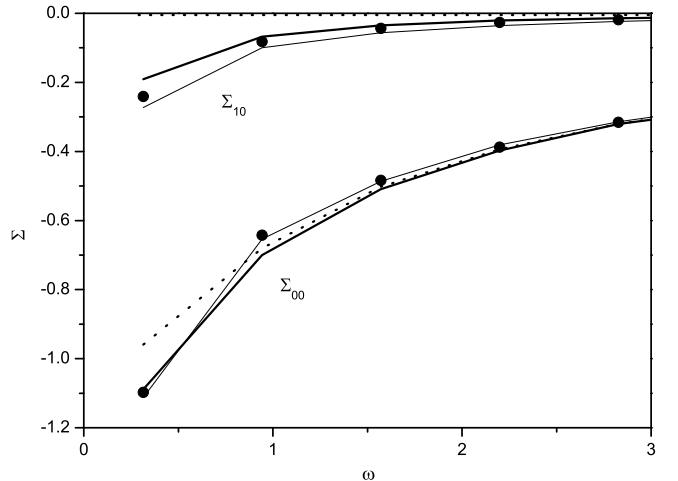


FIG. 2: Local and nearest-neighbor parts of the self energy for half-filled Hubbard model with $U = 2$, $|t| = 0.25$ at $\beta = 10$. Points show the result of lattice QMC simulation. Dot lines show single-impurity DMFT result. Thick solid lines present the result of calculation with diagrams (a) and (b) from Figure 1. Thin lines correspond to the calculation with diagrams (a), (b), (c) and (d). Note that in all cases only the data at Matsubara frequencies are available; lines are drawn to guide the eye. Local part of self energy $\Sigma_{R=(0,0)}$ is described well already in the single-impurity DMFT, but the non-local part of Σ is ignored in this approach, for example $\Sigma_{R=(0,1)}^{DMFT} = 0$. The lowest-order correction describes correctly both $\Sigma_{R=(0,0)}$ and $\Sigma_{R=(0,1)}$. The next correction improves an accuracy.

grew as β increased. Thus we concluded that the formation of pseudogap is entirely related to the non-local part of Σ .

Figure 2 shows the components $\Sigma_{R=(0,0)}$, $\Sigma_{R=(0,1)}$ of the self energy in the space representation for a temperature corresponding to a well-formed pseudogap regime. Figure 3 shows a maximum-entropy estimation [31] for the density of states (DOS) of the same system. The results of the lattice calculation are drawn with circles in this Figure, whereas the dotted lines show the DMFT result. Although the local part of self energy is well described, the DMFT DOS shows an artificial Kondo-like peak at the Fermi level, since the non-local part of Σ is neglected. Solid lines in the same Figure show the data obtained by the diagrams (a) and (b). There is now a dramatic improvement of the DMFT results. The non-local part of Σ now differs from zero and is in a good agreement with the lattice calculations. The pseudogap formation is described quite well. There is only a quantitative underestimation of the pseudogap minimum. To increase the accuracy, the next order diagrams can be considered. The following considerations are helpful to determine what kind of higher-order corrections are the most relevant. Excluding the case of very small U , the physics of antiferromagnetic correlations in half-filled Hubbard model is captured in a simple dimer picture, as

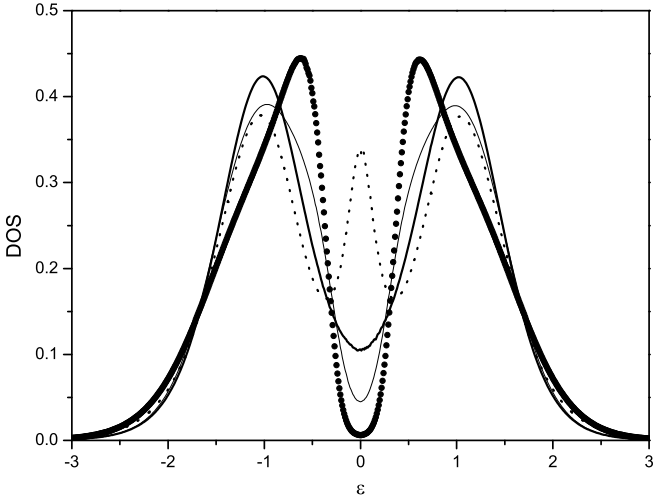


FIG. 3: Density of states for half-filled Hubbard model with $U = 2$, $|t| = 0.25$ at $\beta = 10$. Legend is the same as in Figure 2. At low energy, lattice simulation shows a pseudogap, as $|G(\omega)|$ decreases for small ω . Single-impurity DMFT ignores the effect, whereas already the lowest-order correction describes the physics of the pseudogap correctly.

the tendency is for singlet formation at bonds [32]. This means, that diagrams including only two lattice sites are responsible for the leading corrections. Diagrams (c) and (d) are the simplest examples; other two-site diagrams are similar but contain $\gamma^{(8)}$ and higher-order vertices. The results of calculation with diagrams (a),(b),(c), and (d) included are shown in Figures 2,3 by thin line. The corrections (c) and (d) do improve the results further. In certain sense, a summation of dimer-like diagrams resembles the Dynamical Cluster Approximation method and gives a similar result [33]. However, QMC part of the calculation is much simpler in our method and we do not suffer from the problems of boundary condition in the different cluster-DMFT schemes [14, 32].

It should be noted that, the DMFT solution is not the only choice of ansatz in the expansion of impurity problem. It can be useful to modify somehow a condition for Δ (9). For example, it may be particularly interesting to require the vanishing of the local part of the *renormalized* dual Green function, i.e. to require that diagram (a) is identically zero.

It is important to stress that our approach does not require the summation of an infinite series of diagrams, in contrast with [23, 24]. Moreover, the simplest ladder-like diagrams (e) and (f) from Figure 1 give no remarkable contribution to the self energy, as was checked by our explicit calculations.

To conclude, we have formulated an effective perturbation theory to calculate the momentum dependence of self energy starting with single-site DMFT or any local approximations. The vertices of the effective impurity problem play the role of formal small parameters. Due

to the transformation to dual fermionic variables, consideration of a few leading diagrams provides a quite satisfactory description of the nonlocal correlation effects in a broad range of parameters, up to the atomic limit. This scheme can be easily generalized to multiband case to be implemented into realistic electronic structure calculations for strongly correlated systems.

The work was supported by NWO project 047.016.005 and FOM (the Netherlands), DFG Grant No. SFB 668-A3 (Germany), and Leading scientific schools program and “Dynasty” foundation (Russia).

- [1] J. Hubbard, Proc. Roy. Soc. (London), Ser. A **276**, 238 (1963).
- [2] D.J. Scalapino, Phys. Rep. **251**, 1 (1994); J. Low Temp. Phys. **117**, 179 (1999).
- [3] P.W. Anderson, *The Theory of Superconductivity in High- T_c Cuprates* (Princeton Univ. Press, Princeton, 1997).
- [4] T. Moriya, *Spin Fluctuations in Itinerant Electron Magnetism* (Springer, Berlin, 1985).
- [5] A. Georges *et al*, Rev. Mod. Phys. **68**, 13 (1996).
- [6] G. Modugno *et al*, Phys. Rev. A **68**, 011601(R) (2003); M.Köhl *et al*, Phys. Rev. Lett. **94**, 080403 (2005); J.K. Chin *et al*, Nature **443**, 961 (2006).
- [7] E. Dagotto, Rev. Mod. Phys. **66**, 13 (1994).
- [8] R. Blankenbecler *et al*, Phys. Rev. D **24**, 2278 (1981).
- [9] J.E. Hirsh and R.M. Fye, Phys. Rev. Lett. **56**, 2521 (1986).
- [10] H. De Raedt and A. Lagendijk, Phys. Rev. Lett. **46**, 77 (1981); H. De Raedt and M. Frick, Phys. Rep. **231**, 107 (1993).
- [11] A.C. Hewson, *The Kondo Problem to Heavy Fermions* (Cambridge Univ. Press, Cambridge, 1993).
- [12] A.I. Lichtenstein *et al*, Phys. Rev. Lett. **87**, 067205 (2001).
- [13] G.D. Mahan, *Many-Particle Physics* (Plenum, N. Y., 1993).
- [14] T. Maier *et al*, Rev. Mod. Phys. **77**, 1027 (2005).
- [15] A.I. Lichtenstein and M.I. Katsnelson, Phys. Rev. B **62**, 9283(R) (2000).
- [16] V.Yu. Irkhin *et al*, Phys. Rev. B **64**, 165107 (2001), Phys. Rev. Lett. **89** 076401 (2002).
- [17] J. Schäfer *et al*, Phys. Rev. B **72**, 155115 (2005).
- [18] G. Kotliar *et al*, Phys. Rev. Lett. **87** 186401 (2001).
- [19] M. Potthoff *et al*, Phys. Rev. Lett. **91**, 206402 (2003).
- [20] V.V. Mazurenko *et al*, Phys. Rev. B **66**, 081104(R) (2002).
- [21] A. I. Poteryaev *et al*, Phys. Rev. Lett. **93**, 086401 (2004).
- [22] S. Biermann *et al*, Phys. Rev. Lett. **94** 026404 (2005).
- [23] A. Toshi, A.A. Katanin, and K. Held, cond-mat/0603100.
- [24] H. Kusunosa, cond-mat/0602451.
- [25] Of course, the Bethe-Salpeter equation itself is exact irrespective of the value of U , up to atomic limit. However, the first step of the procedure produces an approximate vertex Γ , which is insufficient in the case of large U .
- [26] J. M. Luttinger and J. C. Ward, Phys. Rev. **118**, 1417 (1960).
- [27] G. Baym and L. P. Kadanoff, Phys. Rev. **124**, 287 (1961).

- [28] N. E. Bickers and D. J. Scalapino, Ann. Phys. (N.Y.) **193**, 206 (1989).
- [29] N.D. Mermin and H. Wagner, Phys. Rev. Lett. **17**, 1133 (1966).
- [30] A. N. Rubtsov *et al*, Phys. Rev. B **72**, 035122 (2005).
- [31] M. Jarrell and J. E. Gubernatis, Phys. Rep. **269**, 133 (1996).
- [32] C. J. Bolech, S. S. Kancharla, and G. Kotliar, Phys. Rev. B **67**, 075110 (2003).
- [33] S. Moukouri and M. Jarrell, Phys. Rev. Lett. **87**, 167010, (2001).